Journal of the Korean Magnetic Resonance Society **2016**, *20*, 95-101
DOI 10.6564/JKMRS.2016.20.3.095

Solution State Structure of P1, the Mimetic Peptide Derived from IgM Antigen Apo B-100 by NMR

Gilhoon Kim, Hyuk Lee, Hyewon Oh and Hoshik Won*

Department of Applied Chemistry, Hanyang University, 55, Hanyang Daehak-Ro, Sangrok-Gu, Ansan 426-791, Republic of Korea

Received Aug 2, 2016; Revised Aug 15, 2016; Accepted Aug 23, 2016

Abstract Apolipoprotein B-100 (Apo-B100) is a major component of low density lipoprotein (LDL). Apo B-100 protein has 4,536 amino acid sequence and these amino acids are classified into peptide groups A to G with subsequent 20 amino acids (P1-P302). The peptide groups were act as immunoglobulin (Ig) antigens which oxidized via malondialdehyde (MDA). The mimetic peptide P1 (EEEMLENVSLVCPKDAT RFK) out of D-group peptides carrying the highest value of IgG antigens were selected for structural studies that may provide antigen specificity. Circular Dichroism (CD) spectra were measured for peptide secondary structure in the range of 190-250 nm. Experimental results show that P1 exhibit partial of β-sheet and random coil structure. Homonuclear (COSY, TOCSY, NOESY) 2D-NMR experiments were carried out for NMR signal assignments and structure determination for P1. On the basis of these completely assigned NMR spectra and distance data, distance geometry (DG) and Molecular dynamics (MD) were carried out to determine the structures of P1. The proposed structure was selected by comparisons between experimental NOE spectra and back calculated 2D NOE results from determined structure showing acceptable agreement. The total Root-Mean-Square-Deviation (RMSD) value of P1 obtained upon superposition of all atoms was in the range 0.33Å. The solution state P1 has mixed structure of β-sheet (Glu[1] to Cys[12]) and random coil (Pro[13] to Lys[20]). These NMR results are well consistent with secondary structure from experimental results of circular dichroism. Structural studies based on NMR may contribute to the studies of atherosclerosis and observed conformational characteristics of apo B-100 in LDL using monoclonal antibodies.

Keywords Apolipoprotein B-100, Immunoglobulin, Molecular dynamic computation, NMR

Introduction

Plasma lipoproteins are water-soluble particles composed of lipids and one or more specific proteins called apolipoproteins.[1] Apolipoproteins playing an important role in lipid transport and metabolic process in blood stream are components of LDL and HDL. Apolipoproteins are classified into A-I, A-II, B, C-I, C-II, D, E, respectively, based on the ABC nomenclature. There are three main lipoprotein classes according to density: very low density lipoproteins (VLDL), low density lipoproteins (LDL, d = 1.019 -1.063 g/mL), and high density lipoproteins (HDL, d = 1.063-1.21 g/mL).[2] Studies relating to the structure and metabolism of LDL are important because of the direct correlation between atherosclerosis and high LDL levels in human plasma. LDL is the end product

* Address correspondence to: **Hoshik Won,** Department of Applied Chemistry, Hanyang University ERICA, 55, Hanyang Deahak-Ro, Sangrok-Gu, Ansan, 426-791, Korea, Tel : 031-400-5497, E-mail: hswon@hanyang.ac.kr

of VLDL catabolism and the major cholesterol-transporting lipoprotein in human plasma. The majority of LDL particles contain a single apolipoprotein called apo B-100.[2,3] After the elucidation of the role of apolipoproteins in the regulation of lipoprotein metabolism, it became apparent that improvements in the characterization of apo B-100 were needed to facilitate the development of the linkage between LDL and atherosclerosis.[2]

Apolipoprotein B is the largest and one of the most important proteins that cover the lipid surfaces of lipoproteins. Apo B exists in two forms, apo B-100 and apo B-48.[4] Apolipoprotein B (apo B) is the major protein component of plasma LDL. It plays functional roles in lipoprotein bio-synthesis in liver and intestine, and is the ligand recognized by the LDL receptor during receptor mediated endocytosis.[5] Apo B-100 which consists of 4,536 amino acids has a molecular mass of 513 kDa and its levels of both LDL-cholesterol and plasma apo B are correlated with coronary heart.[6] The structure of human apo B has been analyzed in term of its functions in lipid binding, lipoprotein assembly and as the ligand responsible for LDL clearance by the LDL receptor pathway.[7-9] In apo B-100 few of the predicted α-helices are truly amphipathic in terms of charge distribution on the polar surface except for one extended region(residues 2,000-2,600) which contains good examples of amphipathic α-helices, and may contribute to lipid binding. The secondary structure of apo B-100 has been suggested to consist of 43% α-helical, 21% β-sheet, 16% β-turn and 20% random structure.[10-12] The β-structure of apo B-100 is thought to be responsible for its interaction with lipids, due to its high hydrophobicity, but is not confined to a particular region and various sections of the protein are buried in the lipid moiety.[13]

Recently, computer modeling studies based upon biochemical analyses have shown that large segment of the apo B backbone have a high amphipathic structure predicted to bind lipid. If these amphipathic β-sheets and α-helices are not folded and associated with lipid in the proper temporal sequence, the structural model predicts that the hydrophobic surfaces would become unstable in the aqueous environment of the ER lumen, leading to improper folding of nascent apo B and eventual degradation.[14,15]

Apo B-100 has 357 lysine residues per molecules, because this protein is intimately associated with lipid in the LDL particles.[16] These lysine residues has highly conjugate with MDA(malondialdehyde) during lipid peroxidation. During the oxidative modification of LDL, conjugation of lipid peroxidation products to apo B occurs primarily covalent linkage to epsilon amino groups of lysine residues. If oxidized LDL contains lysine residues conjugated to a number of such fatty acid fragments, the occurrence of oxidatively modified LDL *in vivo* could be demonstrated by its recognition by mono specific antibodies directed against the various lysine adducts.[7,17]

Conformational studies for mimetic peptide P1(EEE MLENVSLVCPKDATRFK) recognized by the monoclonal antibodies will be discussed from computer simulation analysis in this study.[18,19] 2D-NMR (COSY, TOCSY, NOESY) experiments were performed using peptide. Circular Dichroism (CD) spectra were compared for peptide secondary structure. Electronic circular dichroism (CD) is the most extensively used spectroscopic technique to determine global secondary structural information in peptides and proteins in solution. NMR signal assignments were accomplished by using 2D-NMR experiments. On the basis of these distance data from NOESY experiments, Distance Geometry (DG) and Molecular Dynamics (MD) were carried out to obtain the tertiary structure of mimetic peptide P1.

Experimental Methods

Sample preparation Apo B-100 peptide P1 (EEEML ENVSLVCPKDATRFK) was obtained from Peptron Inc. Peptide was synthesized using solid-phase method. The water soluble P1 was dissolved at 3.20 mM concentration in 400 μL DMSO-d_6 for NMR experiments and 0.24 μM in DMSO-d_6 for Circular dichroism measurement.

NMR experiments All NMR experiments were performed by using the 500MHz Varian spectrometer at

298K. Two-dimensional NMR experiments included COSY and TOCSY, NOESY experiments were performed with a 512 × 2048 data matrix size with 32 scans per t1 increment and spectra were zero filled of 2048 × 2048 data points. TOCSY spectrum was collected with a mixing time of 80 ms, MLEV-17 spin lock pulse sequence. Although NOESY experiments were recorded at two different 300 ms and 400 ms mixing time, the NOE spectrum at 300 ms mixing time was used for signal assignment and 2D-NOE back-calculation. Data were processed and analyzed on a SGI Octane workstation using Felix and NMR View (8.0.b49). NMRView was also used for sequential assignment of each amino acid.

CD measurements Secondary structure of P1 peptide was determined by using Chiralscan-plus spectrophotometer at 298K. Measurements at 190-250nm were made in a 1.0cm quartz cell. CD measurements are reported as mean residue ellipticity at a given wavelength of peptide and sample data were processed using the CDNN (ver2.1).

Solution state structure determination Peptide Structure determinations were carried out using HYGEOM™ and HYNMR™. Sequential assignments of amino acid spin systems were made using TOCSY and NOESY. Most important, direct way for secondary structure determination based on qualitative analysis of NOE spectrum. The structures were calculated from the NMR data according to the standard HYGEOM™ simulated annealing and refinement protocols with minor modifications. Most of distance geometry (DG) algorithm accepts the input of distance constraints from NOE measurements. The structure was calculated using the DG algorithm HYGEOM™, and separated structures were generated using all of the constraints and random input. No further refinement by energy minimization was carried out on the output of the DG calculations. Root mean square distances (RMSD) deviations between the NMR structures were 0.33 Å for the backbone. Back-calculation was assigned to GNOE calculation in order to generate the theoretical NOEs. A consecutive serial files, obtained from GNOE calculation, were incorporated into HYNMR™ to generate NOE back-calculation spectra which can be directly compared with experimental NOESY spectra.[20]

Results

Connectivities derived from through bond J-coupling and through space coupling are important in NMR signal assignment and solution state structure determination. The ^{1}H-^{1}H connectivities that identify the different amino acid type are established via scalar spin-spin coupling, using COSY and TOCSY.

Complete NMR signal assignments listed in Table 1 were accomplished by utilizing homonuclear J resolved 2D NMR experiments. Assignments using sequential NOEs can be obtained for proteins with natural isotope distribution. Relations between protons in sequentially neighboring amino acid residues i and i+1 are established by NOEs manifesting close approach among $d_{\alpha N}$, d_{NN}, $d_{\beta N}$. Except for flexible terminal amino acid residue Pro[13]. The correlating signals of adjacent residues on the basis of dipolar connectivities obtained from 2D NOE spectra are listed in Table 2. Dipolar connectivities from amide protons to α- and amide protons were also used for sequential signal assignments, and the fingerprint region of the NOE spectra recorded at 300 ms are shown in Figure 1. Structure calculation was used to many inter-residue and intra-residue NOE connectivities. Table 2 indicates the important NOE connectivities used for the structure determination. Specific conformation of peptide P1 are observed to be $Glu[1]_{\beta H}$-$Cys[12]_{NH,}$ $Asn[7]_{\alpha H}$-$Val[8]_{NH}$, $Leu[10]_{NH}$-$Cys[12]_{NH}$, $Val[8]_{NH}$-$Leu[10]_{NH}$ Although relatively weak $d_{\alpha N}$(i, i+2) dipolar connectivities from residue number 10 to 12 were observed, it was apparent that the P1 has a characteristic conformation including a β-turn form and random coil. In order to determine the DG structure, several variable velocities simulated annealing and conjugate gradient minimization steps were used in the refinement scheme. Addition of restraints to account for minor differences between experimental and back calculated spectra enabled the generation of new DG structures with substantially reduced penalties. To determine which of the DG structures most accurately reflect the experimental

NOESY data, 2D NOESY back calculations were carried out. As illustrated in Figure 3, back calculated spectrum of the P1 was generally consistent with the experimental NOESY data. 10 final super positioned DG structure are shown in Figure 5.

Table 1. ^{1}H-NMR chemical shifts of P1

Residue	NH	αH	βH	γH	Others
Glu[1]		4.65	2.19 2.07	2.73 2.59	
Glu[2]	8.36	4.56	2.10 1.97	2.64	
Glu[3]	8.42	4.47	2.06 1.95	2.45	
Met[4]	8.17	4.49	2.06 1.93	2.43	
Leu[5]	8.21	4.73	1.81	1.65	δCH_3 : 1.55 δCH_3 : 1.08
Glu[6]	8.79	4.54	2.11 1.98	2.50	
Asn[7]	8.40	4.80	2.78 2.61		
Val[8]	7.98	4.39	2.21		γCH_3 : 1.02
Ser[9]	8.24	4.51	3.79		
Leu[10]	8.28	4.39	1.73		δCH_3 : 1.55
Val[11]	7.82	4.35	2.14		γCH_3 : 1.03
Cys[12]	8.30	4.46	2.99 2.45		
Pro[13]		4.54	2.50 2.28		γCH_2 : 1.41
Lys[14]	7.96	4.38	2.21 1.87		εCH_2 : 2.97 δCH_2 : 1.73 γCH_2 : 1.55
Asp[15]	8.27	4.73	2.90 2.73		
Ala[16]	8.07	4.52			
Thr[17]	7.98	4.39	4.16		γCH_3 : 1.21
Arg[18]	8.02	4.45	1.85		δCH_2 : 3.25 γCH_2 : 1.61
Phe[19]	8.50	4.58	2.93 2.62		
Lys[20]	8.11	4.50	1.81 1.69		δCH_2 : 1.46 γCH_2 : 1.01

Table 2. Important NOE connectivities used for the structure determination of P1

Residue	δ(ppm)	NOE connectivities
$Glu[1]_{\alpha H}$	4.65	$E^{1}{}_{\gamma H}$(w), $E^{1}{}_{\beta H}$(m)
$Glu[2]_{NH}$	8.36	$E^{2}{}_{\alpha H}$(w), $E^{2}{}_{\gamma H}$(w), $E^{2}{}_{\beta H}$(w)
$Glu[2]_{\alpha H}$	4.56	$E^{2}{}_{\beta H}$(m)
$Glu[3]_{NH}$	8.42	$M^{4}{}_{NH}$(w),$E^{3}{}_{\alpha H}$(s),$E^{2}{}_{\gamma H}$,(w)$E^{3}{}_{\beta H}$(w)
$Glu[3]_{\alpha H}$	4.47	$E^{2}{}_{\gamma H}$(w), $E^{3}{}_{\gamma H}$(w), $E^{3}{}_{\beta H}$(m)
$Met[4]_{NH}$	8.17	$L^{5}{}_{\alpha H}$(w),$M^{4}{}_{\alpha H}$(s),$M^{4}{}_{\beta H}$(w), $L^{5}{}_{\gamma H}$(w)
$Met[4]_{\alpha H}$	4.49	$L^{5}{}_{\gamma H}$(w)
$Leu[5]_{NH}$	8.21	$L^{5}{}_{\alpha H}$(w), $M^{4}{}_{\beta H}$(vw)
$Glu[6]_{NH}$	8.79	$E^{6}{}_{\alpha H}$(w), $E^{6}{}_{\beta H}$(w)
$Glu[6]_{\alpha H}$	4.54	$E^{6}{}_{\beta H}$(m)
$Asn[7]_{NH}$	8.40	V_{8NH}(w),$N_{7\alpha H}$(m),$V^{8}{}_{\alpha H}$(w)
$Asn[7]_{\alpha H}$	4.80	$E^{6}{}_{\alpha H}$(w),$V^{8}{}_{\alpha H}$(w),$N^{7}{}_{\beta H}$(w),$E^{6}{}_{\beta H}$(w)
$Val[8]_{NH}$	7.98	$S^{9}{}_{\alpha H}$(w),$V^{8}{}_{\alpha H}$(w),$V^{8}{}_{\beta H}$(w),$L^{10}{}_{\beta H}$(w)
$Val[8]_{\alpha H}$	4.39	$V^{8}{}_{\beta H}$(w)
$Ser[9]_{NH}$	8.24	$S^{9}{}_{\alpha H}$(s), $L^{10}{}_{\beta H}$(w)
$Ser[9]_{\alpha H}$	4.51	$V^{8}{}_{\beta H}$(m), $L^{10}{}_{\beta H}$(vw)
$Leu[10]_{NH}$	8.28	$V^{11}{}_{NH}$(w),$L^{10}{}_{\alpha H}$(s),$S^{9}{}_{\beta H}$(w),$V^{11}{}_{\beta H}$(vw)
$Leu[10]_{\alpha H}$	4.39	$S^{9}{}_{\beta H}$(w), $V^{11}{}_{\beta H}$(w), $L^{10}{}_{\beta H}$(w)
$Val[11]_{NH}$	7.82	$C^{12}{}_{\alpha H}$(w),$V^{11}{}_{\alpha H}$(w),$C^{12}{}_{\beta H}$(w),$V^{11}{}_{\beta H}$(w)
$Val[11]_{\alpha H}$	4.35	$V^{11}{}_{\beta H}$(w), $L^{10}{}_{\beta H}$(w)
$Cys[12]_{NH}$	8.30	$C^{12}{}_{\alpha H}$(w), $P^{13}{}_{\alpha H}$(w)
$Cys[12]_{\alpha H}$	4.46	$P^{13}{}_{\beta H}$(w)
$Pro[13]_{\alpha H}$	4.54	$K^{14}{}_{\alpha H}$(w), $P^{13}{}_{\delta H}$(w), $P^{13}{}_{\beta H}$(w)
$Lys[14]_{NH}$	7.96	$D^{15}{}_{\alpha H}$(m),$P^{13}{}_{\alpha H}$(w),$K^{14}{}_{\alpha H}$(w),$D^{15}{}_{\beta H}$(w)
$Lys[14]_{\alpha H}$	4.38	$K^{14}{}_{\beta H}$(w), $K^{14}{}_{\delta CH2}$(w)
$Asp[15]_{NH}$	8.27	$A^{16}{}_{NH}$(w), $D^{15}{}_{\alpha H}$(w), $K^{14}{}_{\beta H}$(w)
$Asp[15]_{\alpha H}$	4.73	$K^{14}{}_{\alpha H}$(vw), $K^{14}{}_{\varepsilon CH2}$(w), $D^{15}{}_{\beta H}$(w)
$Ala[16]_{NH}$	8.07	$D^{15}{}_{\alpha H}$(w), $A^{16}{}_{\alpha H}$(w)
$Ala[16]_{\alpha H}$	4.52	$T^{17}{}_{\alpha H}$(w)
$Thr[17]_{NH}$	7.95	$D^{15}{}_{\alpha H}$(vw), $A^{16}{}_{\alpha H}$(w), $T^{17}{}_{\alpha H}$(w)
$Thr[17]_{\alpha H}$	4.39	$R^{18}{}_{\beta H}$(w)
$Arg[18]_{NH}$	8.02	$R^{18}{}_{\alpha H}$(m), $T^{17}{}_{\beta H}$(w)
$Arg[18]_{\alpha H}$	4.45	$T^{17}{}_{\beta H}$(w)
$Phe[19]_{NH}$	8.50	$F_{19\alpha H}$(w)
$Phe[19]_{\alpha H}$	4.58	$R^{18}{}_{\delta CH2}$(w), $R^{18}{}_{\beta H}$(w)
$Lys[20]_{NH}$	8.11	$K^{20}{}_{\alpha H}$(s), $K^{20}{}_{\beta H}$(w)
$Lys[20]_{\alpha H}$	4.50	$K^{20}{}_{\beta H}$(w)

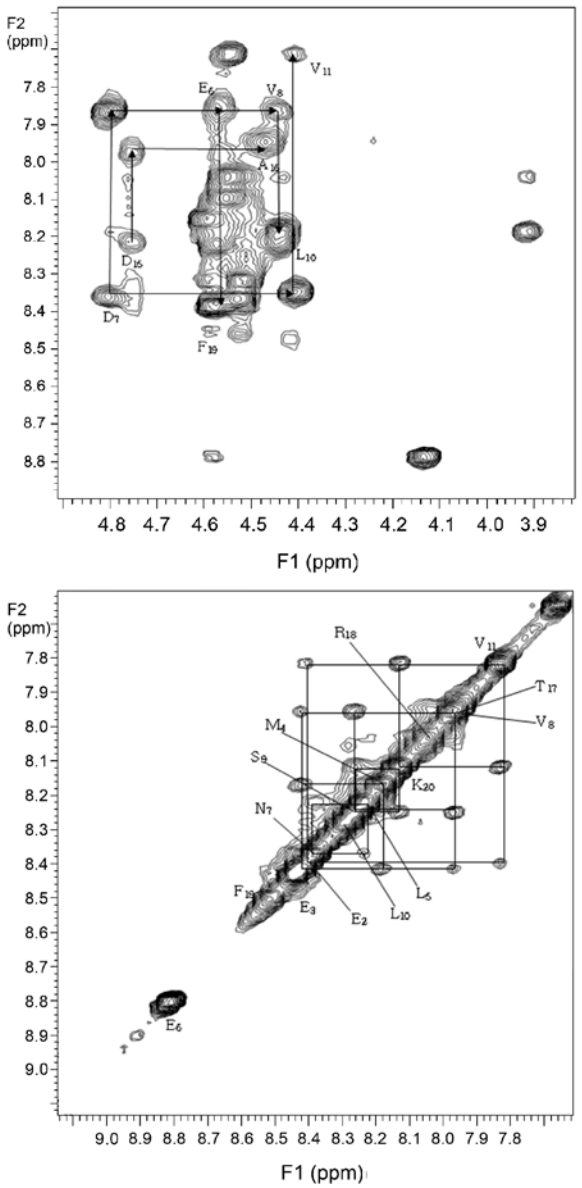

Figure 1. Intra-residue cross peaks labeled in the NH-$C_{\alpha H}$ region (upper), NH-NH region (lower) of the NOE spectra of P1 (τ_m = 300 ms).

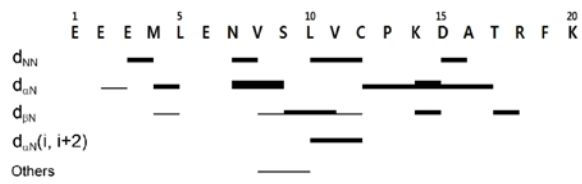

Figure 2. NOESY connectivities involving backbone protons for amino acids i and j. The height of the bars symbolizes the relative strength (strong, medium, weak) of the cross peaks in a qualitative way.

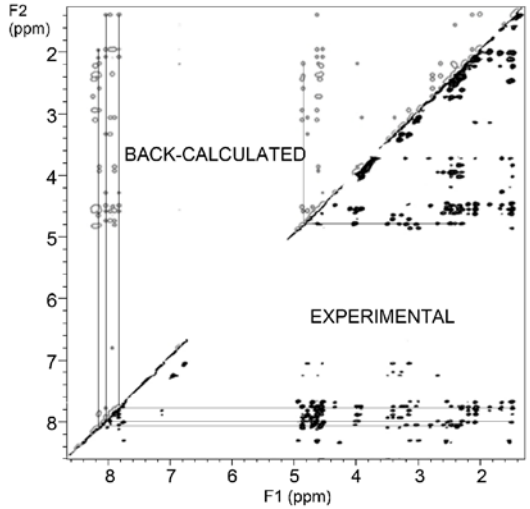

Figure 3. Comparison of back-calculation and experimental NOESY spectrum of P1 collected at 300 ms mixing time.

The secondary structure of P1 was analyzed by CD spectrum as shown in figure 4. Peptide carrying an unique conformational motif shows characteristic CD spectrum. For example, α-helices display large CD bands with negative ellipticity at 222 and 208 nm, and positive ellipticity at 193 nm, β-sheets exhibit a broad negative band near 218 nm and a large positive band near 195 nm, while disordered extended chains have a weak broad positive CD band near 217 nm and a large negative band near 200 nm.[20] The spectrum of a protein is basically the sum of the spectra of its conformational elements.

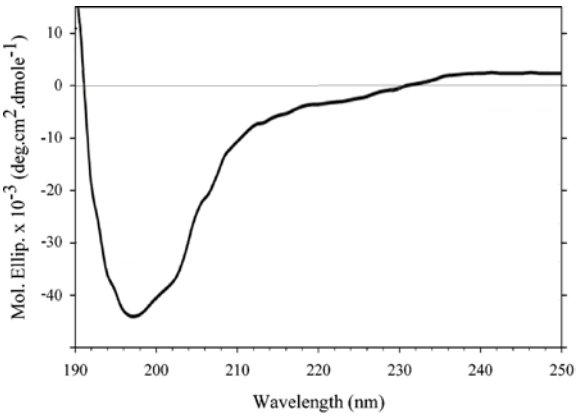

Figure 4. Circular Dichroism spectrum of P1 from 190 to 250nm at 1.0nm intervals.

The result of calculated CD spectra shows that P1 peptide contains conformational ratios like 11.7% of α-helices, 33.9% of anti-parallel, 15.4% of β-sheets, and 29.7% of random coil. Analyzed CD data can be compared and evaluated with our structure model.

Discussion

NMR signal assignments of P1 peptide were made by using homonuclear correlation 2D NMR experiments including COSY, TOCSY and NOESY. Dipolar connectivities from amide protons to α-and amide protons were used for sequential signal assignments. NMR based solution structures were determined with important NOEs and 2D-NOE back calculation method. Out of P1 residues (EEEMLENVSLVCPK DATRFK) $Glu[1]_{\beta}$-$Cys[12]_{NH}$ clearly demonstrate a β-turn conformation as shown in Figure 5. As a result of NMR based structure determination of Apo B-100 partial peptides P1. Pairwise RMSDs obtained upon superposition of all atoms were in the 0.33Å. The final result of a structure determination is presented as a superposition of a group of conformers for pairwise minimum root mean square deviation (RMSD) relative to a predetermined conformer. The secondary structure of proteins was obtained with CD spectra. Experimental result show that P1 has structure of

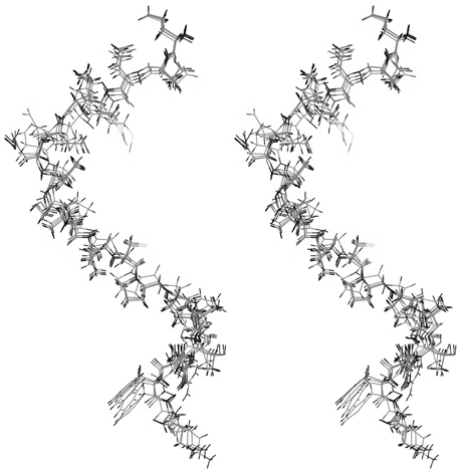

Figure 5. Stereo-views of P1 showing best-fit super positions of all atoms (excluding protons).

β-sheet and random coil.

It was found that peptides have a characteristic β-turn structure possibly derived from the proline in the middle of sequences as compared. It is believed that lysine residue may play important role in the recognition of the monoclonal antibodies in via peroxidation with MDA. Future molecular docking studies with current results may provide the antigen specificity and regulation of surface conformational changes in the mechanism of apolipoproteins playing an important role in lipid transport and metabolic process in blood stream are components of LDL and HDL.

Acknowledgements

This work was supported by the research fund of Hanyang University (HY-2016-G).

References

1. I. D. Cruzado, S. L. Cockrill, C. J. McNeal, and R. D. Macfarlane, *J. Lipid Res.* **39**, 205 (1998)
2. R. W. Mahley, T. L. Innerarity, S. C. Jr. Rall, and K. H. Wesgraber, *J. Lipid Res.* **25**, 1277 (1984)
3. R. A. Davis, *Biochem. Lipid* (1991)
4. B. H. Browman, *Hepatic Plasma Proteins Mechanisms of Function and Regulations,* Academic Press, Inc., London (1993)
5. V. N. Schumaker, M. L. Phillips, and J. E. Chatterton, *Adv. Protein* **45**, 205 (1994)

6. S. H. Chen, C. Y. Yang, P. F. Chen, D. Setzer, M. Tamimura, W. H. Li, A. M. Gotto, and L. J. Chan, *Biol. Chem.* **261**, 12918 (1986)
7. T. J.Knott, R. J.Pease, L. M.Powell, S. C.Wallis, S. C.Rall Jr, T. L. Innerarity, B. Blackhart, W. H. Taylor, Y. Marcel, R. Milne, D. Johnson, M. Fuller, A. J. Lusis, B. J. McCarthy, R. W. Mahley, B. L. Wilson, J. Scott, *Nature* **323**, 734 (1986)
8. M. L. Phillips, and V. N. Schumaker, *J. Lipid Res.* **30**, 415 (1989)
9. A. D. Cardin, and R. L. Jackson, *Biochem. Biophys. Acta.* **877**, 366 (1986)
10. G. C. Chen, S. Zhu, D. A. Hardman, J. W. Schilling, K. Lau, and J. P. Kane, *J. Biol. Chem*. **264**, 14369 (1989)
11. R. A. Davis, R. N. Thrift, C. C. Wu, and K. E. Howell, *J. Biol. Chem.* **265**, 10005 (1990)
12. G. C. Chen, S. Zhu, D. A. Hardman, J. W. Schilling, K. Lau, J. P. Kane, *J. Biol. Chem.*, **264**, 14369 (1989)
13. C. Ettelaie, P. I. Haris, N. J. James, B. Wilbourn, J. M. Adam, and K. R. Bruckdorfer, *Biochem. Biophy. Acta.* **1345**, 237 (1997)
14. C. Y. Yang, S. H. Chen, S. H. Gianturco, W. A. Bradley, J. T. Sparrow, M. Tanimura, W. H. Li, D. A. Sparrow, S. Deloof, M. Rosseneu, F. S. Lee, Z. W. Gu, A. M. Gotto, L. Chan, *Nature* **323**, 738 (1986)
15. H. Jamila, C. H. Chua, J. K. Dickson, Y. Chenb, M. Yana, S. A. Billerb, R. C. Gregga, J. R. Wetteraua, and D. A. Gordana, *J. Lipid Res.* **39**, 1448 (1998)
16. S. W. Law, S. M. Grant, and K. Hlguchi et al, *Proc. Nati. Acad. Sci. U. S. A.* **83**, 8142 (1988)
17. U. Stelnbrecher, *J. Biol. Chem.* **262**, 3603 (1987)
18. S. Lee, D. Kim, H. Kim, Y. Lee, H. Won, *Bull. Korean Chem. Soc*. **25**, 12 (2004)
19. D. Kim, J. Rho, and H. Won, *J. Kor. Magn. Reson. Soc*. **3**, 44 (1999)
20. N. J. Greenfield, *Trac-Trends Anal. Chem*. **18**, 236 (1999)